Hydrogen-induced phase separation in amorphous $Cu_{0.5}Ti_{0.5}$ alloys. II. Thermal evolution

B. Rodmacq and A. Chamberod
Groupe Métallurgie Physique, Service de Physique, Département de Recherche Fondamentale, Centre d'Etudes Nucléaires de Grenoble, 85 X-38041 Grenoble Cédex, France
(Received 26 October 1987)

The thermal evolution of $Cu_{0.5}Ti_{0.5}$ amorphous hydrides has been studied by both calorimetry and neutron-diffraction experiments for different hydrogen contents. At high hydrogen contents, real-time neutron experiments performed during heating at a constant rate show that long-range crystallization into copper and titanium hydride takes place at a well-defined temperature, as confirmed by the exothermic peak in calorimetry. The onset of desorption of hydrogen at high temperature leads to the formation of metastable Cu-rich and then stable γ-CuTi phases. At smaller hydrogen contents, the evolution is much more gradual. Cu and TiH_x diffraction lines progressively appear in the diffraction pattern. In the meantime the small-angle maximum shifts towards the origin. Crystallization into γ-CuTi proceeds in two stages. In the first one, unusual variation of the lattice parameters is observed, whereas the size of the crystallites is constant. The second one coincides with the decomposition of titanium hydride upon desorption of hydrogen. Such variations are compared to those extracted from small-angle neutron scattering experiments.

I. INTRODUCTION

In the preceding paper[1] (hereafter referred to as Paper I) detailed x-ray and neutron scattering experiments have shown that the introduction of hydrogen in $Cu_{0.5}Ti_{0.5}$ glasses led to a microphase separation between copper and titanium hydride. In this second paper we examine the thermal evolution of $(Cu_{0.5}Ti_{0.5})H_{0.84}$ and $(Cu_{0.5}Ti_{0.5})H_{0.43}$ alloys as followed by both calorimetry and neutron diffraction. Although a large number of papers have already been devoted to both the structure and crystallization behavior of these glassy hydrides,[2–6] our study is motivated by the fact that there is some controversy about the identification of the various signals observed in calorimetry experiments for samples with different hydrogen contents. The advantage of the technique used here is that neutron-diffraction spectra are recorded during heating at a constant rate. By a suitable choice of the range of scattering angles and wavelength, it is thus possible to follow simultaneously the thermal evolution of both the low-angle maximum (resulting from the phase separation) and the higher-angle region (first peaks of the interference function), thus covering the main regions of interest of the scattering. Since these two regions have been shown in Paper I to give complementary information on the nature and extent of phase separation in glassy Cu-Ti hydrides, it will be easier to correlate any modification of the scattering curve with the corresponding exothermic or endothermic events observed by calorimetry.

The main results published up to now on the crystallization behavior of Cu-Ti-H glasses have been concerned with a simultaneous interpretation of differential scanning calorimetry (DSC) and x-ray diffraction experiments. Maeland *et al.*[2,3] studied $CuTiH_{1.33}$ glasses (i.e., $Cu_{0.5}Ti_{0.5}H_{0.665}$) and observed two exothermic peaks at 433 and 508 K and an endothermic reaction at 808 K in calorimetry experiments with a heating rate of 25 K min^{-1}. From x-ray diffraction studies on samples heated at various temperatures for different times, they attributed the exothermic effects to a decomposition of the glassy hydride into copper and titanium hydride and the high-temperature endothermic effect to the reaction of Cu with TiH_x leading to the formation of the stable γ-CuTi phase and to the desorption of hydrogen.

A different interpretation of the low-temperature exothermic effect has been given by Dunlap and Dini[4] on the basis of differential thermal analysis and x-ray diffraction experiments on electrolytically charged $(Cu_xTi_{1-x})H$ alloys ($x=0.4$, 0.5, 0.6). In this case, no evidence of crystallization was found after heating above the first exothermic peak. They concluded that this peak would correspond to some structural change in the amorphous structure, as shown by a shift of the x-ray diffraction peaks to higher angles. In addition, they also observed a supplementary exothermic signal starting at about 640 K and consisting of several small peaks. This signal was attributed to the formation of Cu and TiH_x on the basis of the x-ray results.

Finally, detailed investigations by Bowman *et al.*[5] and Furlan *et al.*[6] confirmed previous results[2,3] and pointed out the much reduced thermal stability of these amorphous Cu-Ti hydrides as compared to both amorphous Cu-Ti alloys and crystalline Cu-Ti hydrides.

While the results which we present in our paper also confirm such a low thermal stability of the amorphous Cu-Ti hydrides, they give a detailed picture of the evolution of the structure from the small-scale phase separation at room temperature to the long-range crystallization of Cu and TiH_x and finally to the appearance of the stable γ-CuTi phase at high temperature, through a continuous recording of the neutron-diffraction spectra dur-

ing heating.[7] Although just a few well-defined transformations can be identified in the case of large hydrogen contents, the thermal evolution is more complicated for smaller hydrogen contents. In this case, such real-time neutron experiments allow one to follow accurately the proportions and crystallographic parameters of the successive phases. It is also possible to correlate these transformations with those observed previously by small-angle scattering on similar samples.[8]

II. EXPERIMENT

The procedure of preparation of the amorphous $Cu_{0.5}Ti_{0.5}$ alloys and of hydrogenation is identical to that described in paper I. Alloys of composition $(Cu_{0.5}Ti_{0.5})H_{0.84}$ and $(Cu_{0.5}Ti_{0.5})H_{0.43}$ were obtained with electrolysis times of 20 and 4 h, respectively. DSC experiments were performed on a DSC-2C calorimeter (Perkin-Elmer) at a heating rate of 20 K min^{-1} under He atmosphere.

Neutron scattering experiments were performed on the high-resolution D1B diffractometer at Institut Laue Langevin (Grenoble) using a wavelength of 2.52 Å. Diffraction spectra were recorded for 5 min each during heating under vacuum with a constant rate of 0.7 K min^{-1} between 295 and 920 K on a q range from 0.17 to 3.3 $Å^{-1}$ ($q = 4\pi \sin\theta/\lambda$). For such a heating rate, these real-time neutron experiments[9] make it possible to follow quite accurately any structural transformation in the sample. In addition, the intense background due to the large incoherent scattering cross section of hydrogen gives precise information on the hydrogen content of the sample at every temperature. Diffraction peaks were fitted to a Gaussian shape in order to extract their position, width, and integrated intensity.[10]

III. $(Cu_{0.5}Ti_{0.5})H_{0.84}$ ALLOYS

Figure 1(a) presents the DSC curve of a $(Cu_{0.5}Ti_{0.5})H_{0.84}$ alloy. Two main features can be observed, an exothermic peak at 390 K with a heat of transition of -15 kJ mol^{-1} and a large endothermic deviation starting at about 750 K and extending over more than 250 K. Compared to previous results on pressure charged samples[6] the exothermic peak appears at a lower temperature for these electrolytically charged samples, as also observed in Ref. 4. This is confirmed by the DSC curve of Fig. 1(b) for a pressure charged sputtered $Cu_{0.5}Ti_{0.5}$ sample.[1] At the same heating rate the exothermic peak is now located at around 460 K. It also appears that the endothermic signal extends over a smaller temperature range. Despite these slight differences (possibly due to the different hydrogen content between both samples), both DSC curves are essentially the same, which implies that the samples are similar, as we also concluded from scattering experiments.[1]

Figure 2 gives some general information about the time and temperature stability of a $(Cu_{0.5}Ti_{0.5})H_{0.08}D_{0.76}$ alloy. These large-angle neutron scattering curves were preferred to those of a hydrogenated sample because of the much smaller incoherent background for deuterated sam-

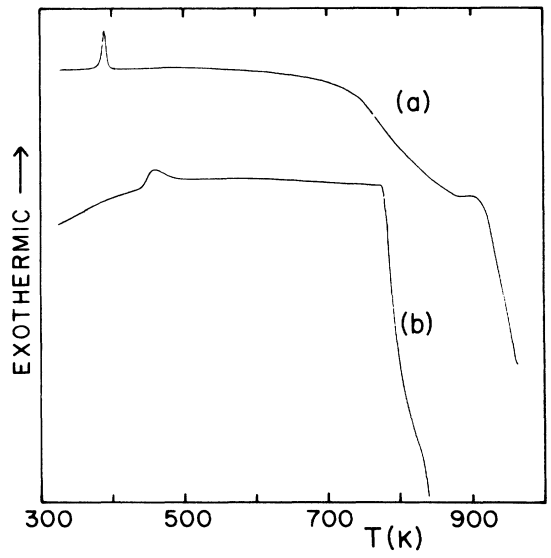

FIG. 1. DSC traces of $(Cu_{0.5}Ti_{0.5})H_{0.84}$ amorphous alloys loaded in hydrogen (a) by electrolysis or (b) from the gas phase. (Hydrogen content is slightly smaller in the second case.)

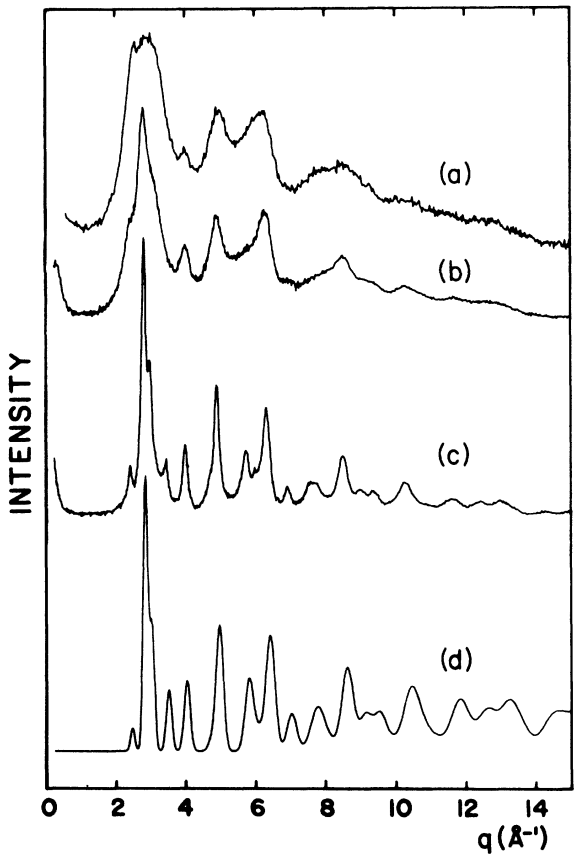

FIG. 2. Evolution of the large-angle neutron diffraction spectra of (a) $(Cu_{0.5}Ti_{0.5})H_{0.08}D_{0.76}$, (b) same as (a) but kept one year at room temperature, (c) same as (a) but after heating to 473 K. Spectrum (d) is a calculated spectrum for a mixture of fcc Cu and $Ti(H_{0.16}D_{1.52})$.

ples. Let us mention that no difference is observed in the DSC curves between both samples. Figures 2(a)–2(c) present the scattering curves of the as-charged sample [Fig. 2(a)] and of the same sample kept one year at ambient temperature [Fig. 2(b)] or heated up to 473 K [Fig. 2(c)], that is above the exothermic peak in Fig. 1(a). The progressive evolution of the curves from Figs. 2(a) to 2(c) supports our conclusions drawn in paper I, that is the broad diffraction peaks for the initial sample sharpen without changing their position or relative intensities (very slowly during long annealing at ambient temperature or very rapidly during heating), indicating that the small-scale phase separation at room temperature transforms into a long-range crystallization. The bottom curve in Fig. 2 is a simulated scattering curve for a mixture of fcc Cu and $Ti(H_{0.16}D_{1.52})$ crystals. The almost perfect coincidence between both curves definitely shows that the low-temperature exothermic peak is related to the crystallization of the sample.

Figure 3 presents the evolution of the scattered intensity as a function of momentum transfer q and temperature T between 295 and 920 K. According to the main changes observed, the temperature range can be divided into four regions, region I from 295 to 360 K, region II from 360 to 670 K, region III from 670 to 800 K, and region IV from 800 to 920 K.

In region I, the main features of the curves are an intense flat background due to the large incoherent scattering cross section of hydrogen with a small-angle maximum at about 0.4 $Å^{-1}$. Owing to the rather short (5 min) counting time for each individual spectrum it is difficult to see the characteristic features of the amorphous hydride at about 3 $Å^{-1}$ (see Fig. 4(c) in Paper I for example). The important point to be noted is that there is no change of the diffraction curves in this temperature range, and particularly no displacement of the low-angle maximum. Since its position is related to the extent of phase separation in the alloy, this means that this phase separation is stable in this temperature range.

At 360 K this maximum suddenly shifts towards the origin whereas sharp diffraction peaks appear, the largest ones at 2.44 and 3.0 $Å^{-1}$ corresponding to the (111) reflections of fcc TiH_x and Cu, respectively. The background decreases slightly at the same temperature because of the decrease of the diffuse scattering (incoherent Laue scattering[11]) upon crystallization. In region II both background and intensity of the diffraction peaks are constant.

At the beginning of region III ($T=670$ K), hydrogen starts desorbing as shown by the decrease of the background. In the meantime the intensity of both TiH_x and Cu peaks start decreasing, whereas at 730 K new sharp lines appear, corresponding to the tetragonal γ-CuTi phase[12] (strongest peaks at 1.05, 2.25, and 3.01 $Å^{-1}$). In the temperature range from 670 to 730 K, the intensity of the Cu phase decreases more rapidly than that of the TiH_x phase, and a supplementary peak appears at 3.11 $Å^{-1}$. Its intensity is maximum at 730 K and then decreases. Although it is difficult to identify this metastable phase because of the weak intensity of its diffraction pattern, it could correspond to a Cu-rich Cu-Ti phase, probably Cu_3Ti or Cu_4Ti.[12,13] Furlan *et al.*[6] also observed the appearance of this metastable phase in their x-ray experiments.

From the position of the diffraction peaks of the γ-CuTi phase one can calculate the lattice parameters a and c. It appears that from 730 to 800 K (i.e., during the growth of this γ phase) parameter a decreases and parameter c increases with increasing temperature. Although such a variation could be attributed to some hydrogen desorption from the γ phase,[6] this seems unlikely since this hydride phase is not stable at such a high temperature. Another explanation could be that the observed simultaneous decrease of the intensity of the metastable Cu-rich phase leads to some change in the stoichiometry of the γ phase.

This structural evolution lasts up to 800 K, at which temperature there are no TiH_x- and Cu-rich phases left. In region IV both background and intensity of the γ-CuTi phase are constant and its lattice parameters both increase normally with temperature. To summarize, the successive reactions identified in the neutron scattering curves can be written

$$(Cu_{0.5}Ti_{0.5})H_{0.84} \xrightarrow{360\ K} Cu + TiH_x ,$$

$$Cu + TiH_x \xrightarrow{670\text{–}730\ K} Cu + Cu_3Ti + TiH_x + H_2 ,$$

$$Cu + Cu_3Ti + TiH_x \xrightarrow{730\text{–}800\ K} \gamma\text{-CuTi} + H_2 .$$

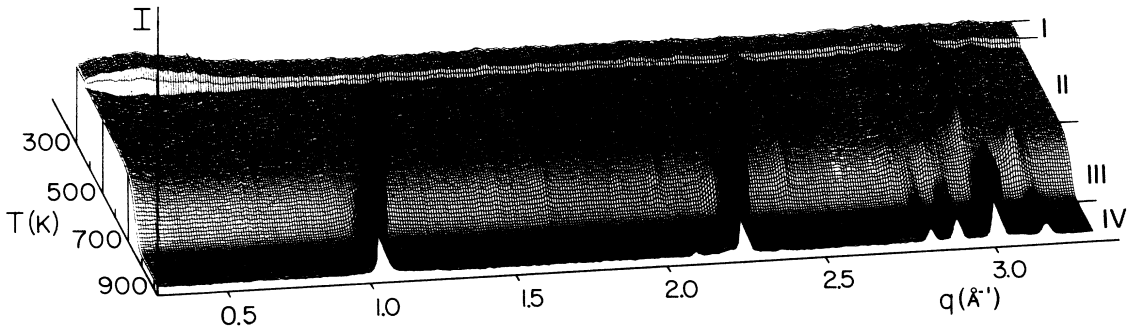

FIG. 3. Thermal evolution of the neutron scattering curves for $(Cu_{0.5}Ti_{0.5})H_{0.84}$ alloys.

Owing to the different heating rates, these neutron-diffraction results are in agreement with those obtained from the DSC experiments [Fig. 1(a)]. Transformation temperatures derived from the neutron experiments are lower according to the smaller heating rate. Moreover the irregular shape of the endothermic signal between about 800 and 900 K can be related to the formation of the metastable Cu_3Ti phase.

IV. $(Cu_{0.5}Ti_{0.5})H_{0.43}$ ALLOYS

A. General evolution

Amorphous alloys with a smaller hydrogen content have a different thermal behavior. Concerning the DSC curves, the low-temperature exothermic peak is no longer present but is replaced by several smaller peaks at higher temperature. As was the case in Fig. 1(a) a strong endothermic effect is also observed at high temperature.

The thermal evolution of the neutron scattering curves in Fig. 4 is also more complicated. The temperature range can be roughly divided into five regions.

Region I (295–410 K): A weak maximum is observed at a small angle ($q \simeq 0.55$ Å^{-1}).

Region II (410–630 K): This maximum starts shifting towards a smaller angle. In the meantime the diffraction lines of Cu and TiH_x progressively grow above the background (difficult to see on the figure).

Region III (630–760 K): Diffraction peaks of γ-CuTi appear suddenly at 630 K. The Cu and TiH_x peaks are also more visible from this temperature. The background is still constant.

Region IV (760–870 K): Hydrogen starts desorbing. Except for the fact that the onset of hydrogen desorption is at higher temperature than for the preceding sample (Fig. 3), the evolution is similar.

Region V (870–920 K): Both background and intensity of the γ-CuTi phase are constant.

Such an evolution reveals important differences compared to the one observed at larger hydrogen contents. The structure at room temperature corresponds to a phase separation at a smaller scale, according to the larger q value of the maximum. Such a structure is equally stable up to 410 K (to be compared to 390 K in the first case). From this temperature up to 630 K, the small-angle maximum progressively shifts to smaller angle, indicating that now the longer-range phase separation extends on a large temperature range. This also corresponds to a progressive sharpening of the diffraction peaks, and explains why such a process is not seen in calorimetry experiments. At 630 K part of the sample crystallizes into γ-CuTi, some 10 K lower than the crystallization temperature of the pure amorphous Cu-Ti alloy at such a heating rate. This shows that, as the phase separation proceeds in region II, parts of the sample are enriched in hydrogen (TiH_x-like regions) whereas other parts are depleted in hydrogen (Cu-like and amorphous regions). But this does not inevitably mean that such nonhydrogenated amorphous regions already exist at room temperature as a consequence of the charging procedure.[6]

Concerning region III between 630 and 760 K, an important point to be noted is that, although the proportion of the γ-CuTi phase is constant in this region, there are noticeable changes in the position of the diffraction peaks, not simply due to the temperature increase. We will go back to this point in the following section.

In region IV hydrogen starts desorbing, as was the case in the other sample. Desorption starts at a slightly higher temperature (760 K instead of 730 K) and also extends over a larger temperature range. It is accompanied by the formation of the metastable Cu_3Ti and stable γ-CuTi phases.

To illustrate the above discussion, Fig. 5 presents the thermal evolution of the background and of the intensities of the (111) reflection of the TiH_x phase and of the (001) reflection of the γ-CuTi phase. The different regions can be easily identified in this figure. One can also note that the accuracy of the intensity of the TiH_x phase is quite low, because of the width of the peaks and of the limited q range studied. [We also recall the short (5 min) accumulation time for each diffraction spectrum.] We will now study in more detail the high-temperature region ($T > 630$ K) through an analysis of the behavior of the γ-CuTi phase since its parameters can be determined with good accuracy.

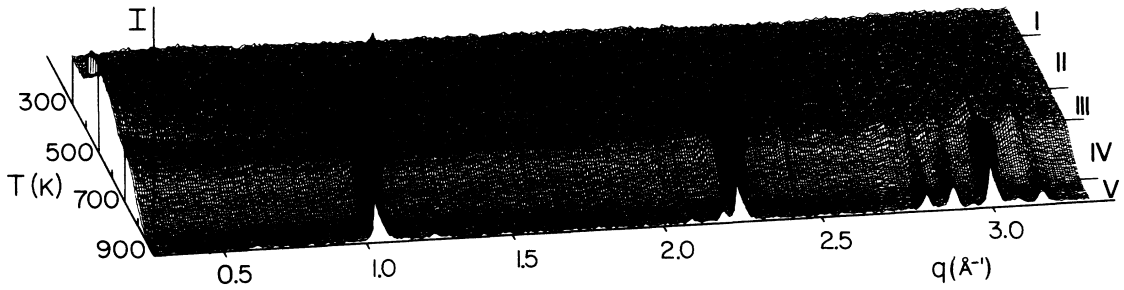

FIG. 4. Same as in Fig. 3 for $(Cu_{0.5}Ti_{0.5})H_{0.43}$ alloys.

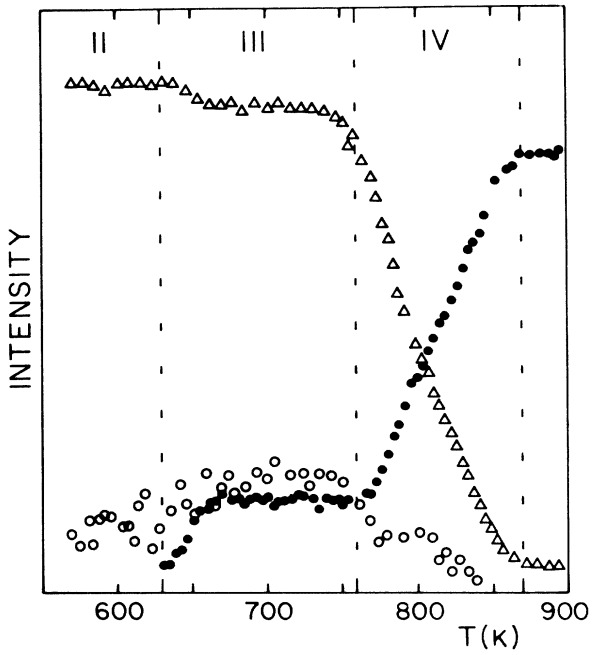

FIG. 5. Thermal evolution of the background (triangles), intensity of the (111) diffraction peak of TiH_x (open circles) and of the (001) diffraction peak of γ-CuTi (solid circles) for $(Cu_{0.5}Ti_{0.5})H_{0.43}$ alloys.

B. Thermal evolution of the γ-CuTi phase

We will focus on an analysis of the two main peaks of this γ-CuTi phase, the (001) reflection at 1.05 $Å^{-1}$ and (011) reflection at 2.25 $Å^{-1}$. To begin with, Fig. 6 shows the thermal variation of the integrated intensity, position and width of the (001) reflection. Note that the position of this peak is not corrected for the thermal variation. As we mentioned above, the γ-CuTi phase appears at 630 K. From about 660 to 760 K (region III) its intensity is constant, and increases again from 760 to 870 K (region IV). In the same temperature intervals, the width of the (001) peak is constant in region III and then decreases in region IV. The variation of the position of this peak is quite unexpected. From Fig. 6 it appears that it shifts to a higher scattering vector as the temperature increases in region III, indicating a decrease of the lattice parameter c of the tetragonal phase, in spite of the thermal expansion. This peak then rapidly shifts to a smaller scattering vector beyond 760 K (region IV). Similar effects are observed for the thermal evolution of the (011) reflection at 2.25 $Å^{-1}$ (curves not shown).

From the thermal variation of both (001) and (011) reflections one can extract the evolution of both a and c parameters of the γ-CuTi phase (corrected for the thermal variation as estimated during cooling of the sample down to room temperature) and of the average size of the γ-CuTi crystals estimated from the Scherrer formula.[14] Figure 7 presents the variation of these parameters, to be compared to that of the incoherent background (i.e., hydrogen content, Fig. 5) and of the intensity of the γ-CuTi phase (Fig. 6).

From this figure it clearly appears that parameter a *increases* and parameter c *decreases* as the temperature increases from 630 to 760 K. In the meantime both intensity of the γ phase and size of the crystallites ($L \simeq 250$ Å) are *constant* in this region. Such a behavior implies some structural modification of the γ phase. From 760 K hydrogen starts desorbing, as indicated by the decrease of

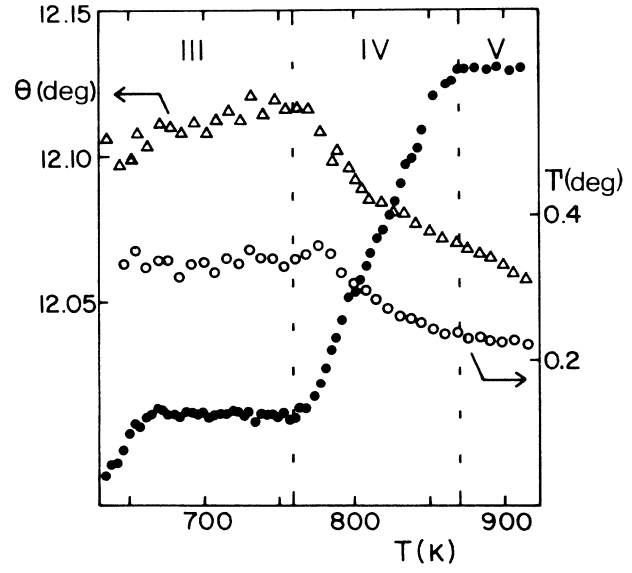

FIG. 6. Thermal evolution of the intensity (solid circles), position θ (triangles, left-hand scale) and width Γ (open circles, right-hand scale) of the (001) peak of the γ-CuTi phase.

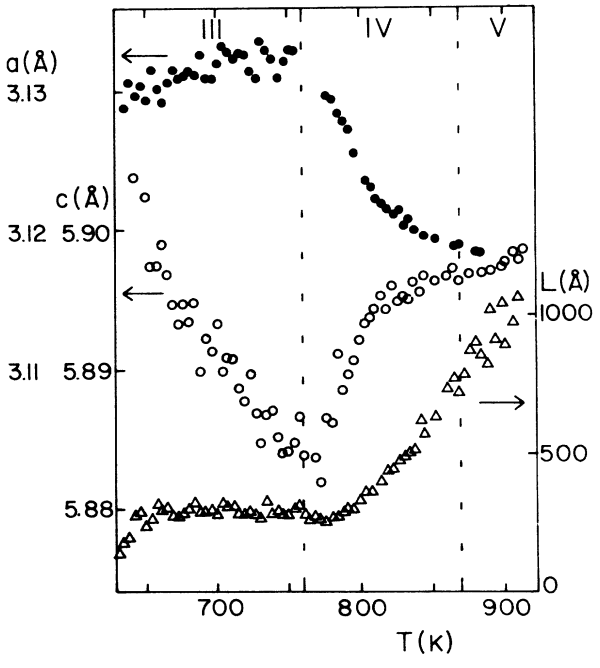

FIG. 7. Thermal evolution of the size of the γ-CuTi crystallites (L) (triangles, right-hand scale) and of the lattice parameters a and c (solid and open circles, left-hand scales).

the background (and also by the decrease of the intensity of the TiH_x reflections, Fig. 5). Both intensity of the γ phase and size of the crystallites increase rapidly in this region, whereas the lattice parameters vary now in a direction opposite to the one in region III. This evolution is similar to the one observed for large hydrogen contents in the same temperature range (Sec. III). The rapid increase of the size of the crystallites is indicative of a long-range reorganization of the γ phase until there is no hydrogen left in the sample.

Although the evolution of the lattice parameters of the γ phase in both regions III and IV corresponds to a slight volume decrease of the atomic cell (-0.14% and -0.60%, respectively) it is clear from Fig. 7 that the origin of this decrease is different in each case since it results from a decrease of parameter c in region III and of parameter a in region IV. We suggested in Sec. III that in region IV the reason could be some change of the stoichiometry of the γ phase. Such an explanation cannot hold in region III since the intensity of the diffraction peaks, and hence the structure factor, is constant here.

Such a behavior in the temperature range from 630 to 870 K (regions III and IV) can be compared to the one observed in small-angle ($0.8\times10^{-2}<q<6.3\times10^{-2}$ Å^{-1}) neutron scattering experiments previously performed on similar Cu-Ti-H glasses.[8] These samples (with a smaller hydrogen content as that of the samples studied here) were studied during heating with the same heating rate between 300 and 800 K. In the temperature range from 645 to 800 K, the intense small-angle upswing was interpreted as arising from fractal aggregates, and the scattering curves could be well fitted to a scattering function corresponding to a correlation function of the form $g(r)=r^{D-3}e^{-r/\xi}$ where D is the fractal dimension of the aggregates and ξ their correlation length. From the thermal variation of both parameters D and ξ (Fig. 8), three regions could be identified, corresponding to the formation ($T<680$ K), restructuring ($680<T<740$ K), and growth ($T>740$ K) of the fractal aggregates. Comparing this evolution to that described above for the large-angle scattering results (Fig. 7), there is a great similarity between both evolutions, although the limits of the different regions are slightly different (as a possible consequence of the different hydrogen content). The region of formation of the fractal aggregates coincides with the appearance of the γ phase, that of the restructuring ($D=2.1$ to $D=3$) of the aggregates at constant correlation length corresponds to a simultaneous variation of the lattice parameters at constant size of the crystallites, and finally that of the growth of compact ($D=3$) aggregates is parallel to the growth of the γ phase and rapid increase of the crystallite size. Although we attributed the small-angle events to TiH_x aggregates in a Cu-Ti matrix, one must recall that the appearance of a small-angle signal results from a contrast difference between regions in the sample.[15] The system is thus completely symmetrical from this point of view. This means that the same evolution should be observed for the TiH_x phase. Unfortunately the weak intensity of the TiH_x peaks in the q range studied does not allow a precise determination of the behavior of this phase.

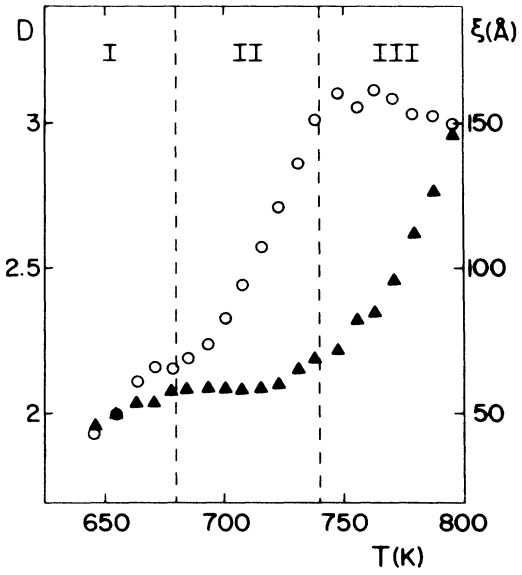

FIG. 8. Thermal variation of the fractal dimension (open circles, left-hand scale), and correlation length (triangles, right-hand scale) as obtained from small-angle neutron experiments (reproduced from Ref. 8).

V. CONCLUSION

These studies of the thermal evolution of Cu-Ti-H glasses confirm the results presented in Paper I about the phase separation between Cu and TiH_x and show that this hydrogen-induced phase separation is metastable at room temperature and evolves towards a long-range crystallization at a well-defined temperature.

In the case of high hydrogen contents, this evolution takes place within a very narrow temperature range and corresponds to the exothermic peak in DSC experiments. At still higher temperature, hydrogen desorption leads to the decomposition of titanium hydride and formation of metastable Cu-rich and stable γ-CuTi phases.

For smaller hydrogen contents, such an evolution is much more gradual, as indicated by the progressive shift of the low-angle maximum towards the origin. The γ-CuTi phase crystallizes into two steps, the first one probably corresponding to the crystallization of the remaining amorphous phase. The second one coincides with the onset of hydrogen desorption, as in the case of large hydrogen contents. A detailed study of the evolution of this γ phase reveals that these two steps correspond to stages of restructuring and growth. A great similarity is found with previous small-angle neutron experiments on samples with a low hydrogen content, which showed successive densification at constant size and growth of fractal aggregates.

ACKNOWLEDGMENTS

The help of Dr. Ph. Goudeau and Dr. J. Pannetier during this work is greatly appreciated.

[1]B. Rodmacq, M. Maret, J. Laugier, L. Billard, and A. Chamberod, preceding paper, Phys. Rev. B **38**, 1105 (1988).
[2]A. J. Maeland, L. E. Tanner, and G. G. Libowitz, J. Less-Common Met. **74**, 279 (1980).
[3]A. J. Maeland, in *Metal Hydrides,* edited by G. Bambakidis (Plenum, New York, 1981), p. 177.
[4]R. A. Dunlap and K. Dini, J. Phys. F **14**, 2797 (1984).
[5]R. C. Bowman, Jr., R. J. Furlan, J. S. Cantrell, and A. J. Maeland, J. Appl. Phys. **56**, 3362 (1984).
[6]R. J. Furlan, G. Bambakidis, J. S. Cantrell, R. C. Bowman, Jr., and A. J. Maeland, J. Less-Common Met. **116**, 375 (1986).
[7]B. Rodmacq, Ph. Goudeau, J. Pannetier, and A. Chamberod, Proceedings of the 6th International Conference on Rapidly Quenched Metals, Montreal, 1987 [Mater. Sci. Eng. (to be published)].
[8]Ph. Mangin, B. Rodmacq, and A. Chamberod, Phys. Rev. Lett. **55**, 2899 (1985).
[9]J. Pannetier, Chem. Scr. **26A**, 131 (1986).
[10]P. Wolfers (unpublished).
[11]C. H. de Novion, in *L'Ordre et le Désordre dans les Matériaux,* edited by N. Clement, J-J. Couderc, and F. Reynaud (les Editions de Physique, Paris, 1984), p. 243.
[12]N. Karlsson, J. Inst. Met. **79**, 391 (1951).
[13]H. U. Pfeifer, S. Bhan, and K. Schubert, J. Less-Common Met. **14**, 291 (1968).
[14]See, for example, H. P. Klug and L. E. Alexander, *X-Ray Diffraction Procedures* (Wiley, New York, 1974), p. 656.
[15]G. Porod, in *Small Angle X-Ray Scattering,* edited by O. Glatter and O. Kratky (Academic, London, 1982), p. 17.

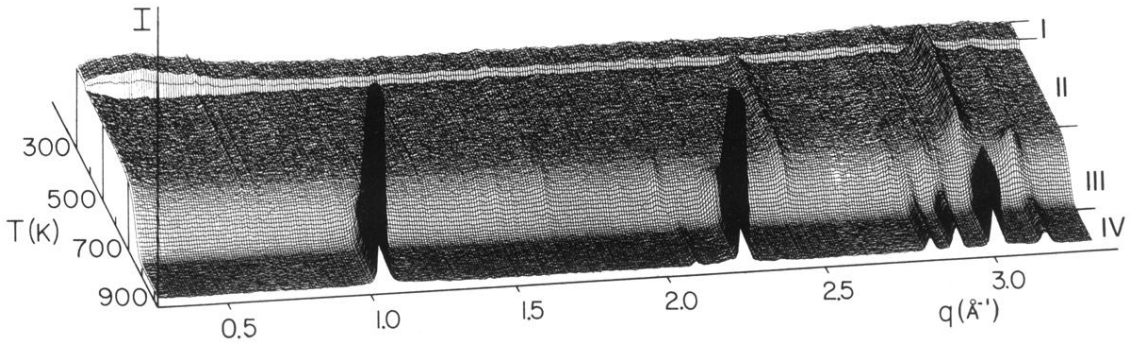

FIG. 3. Thermal evolution of the neutron scattering curves for $(Cu_{0.5}Ti_{0.5})H_{0.84}$ alloys.

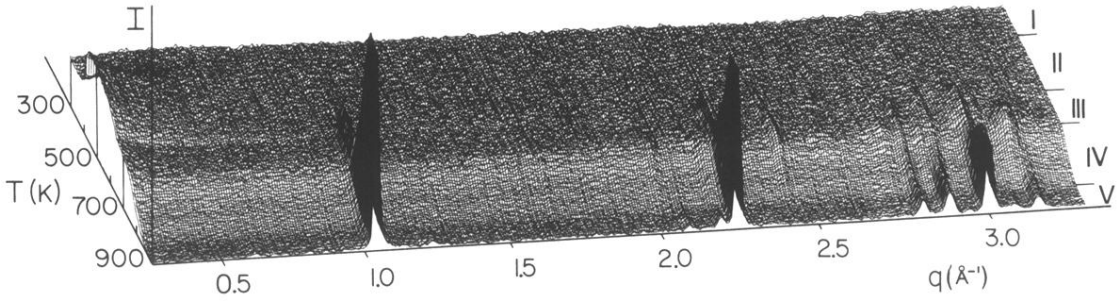

FIG. 4. Same as in Fig. 3 for $(Cu_{0.5}Ti_{0.5})H_{0.43}$ alloys.